

# Comparison of Optimal Control Approximations by Mechanical Impedance Adjustment for a Wave Energy Converter<sup>\*</sup>

Alejandro González-Esculpi<sup>\*</sup> Cristina Verde<sup>\*</sup>  
Paul Maya-Ortiz<sup>\*\*</sup>

<sup>\*</sup> *Instituto de Ingeniería, Universidad Nacional Autónoma de México,  
Circuito Exterior S/N, 04510, Ciudad de México  
(agonzaleze@iingen.unam.mx; verde@unam.mx)*

<sup>\*\*</sup> *Facultad de Ingeniería, Universidad Nacional Autónoma de México,  
Circuito Exterior S/N, 04510, Ciudad de México (paulm@unam.mx)*

---

**Abstract:** This work compares three methods for efficiency improvement of a point absorber wave energy converter (WEC) with approximated optimal control by adjusting the mechanical impedance of the floater dynamics. The case study is a WEC based on an Archimedes wave swing prototype. The well-established phase and amplitude conditions for floaters in the frequency domain are considered as guidelines for the efficiency improvement objective for a floater with nonlinear damping. The phase condition is considered to be fulfilled by matching the natural frequency of oscillation with the dominant frequency of the incident waves. This is a feature of the mechanical structure of the WEC under study. Thus, the three methods considered aim to satisfy the amplitude condition for the WEC under study. These methods seek to correct the total damping by shaping the force produced by the electrical generator. The first method considers a linear approximation of the nonlinear damping produced by the brakes in the WEC structure. The second method imposes a linear dynamic by compensating the nonlinear damping. Finally, the third method is proposed following a variation for nonlinear resistive networks of the maximum power transfer theorem. From numerical simulations with both regular and irregular sea waves, including a sensitivity analysis of the corrected damping, the third option shows a better performance regarding energy conversion followed by the first option.

*Keywords:* Wave energy, renewable energy sources, electromechanical systems, maximum power transfer.

---

## 1. INTRODUCTION

The sea waves represent an important renewable energy source since their global potential has been estimated to be around 32,400 TWh per year (Mork et al., 2010). Despite the lack of consensus on a specific topology for wave energy converters (WECs), the point absorbers (PAs) are an important class because of their simplicity. These devices capture the energy from the waves through a floater of negligible dimensions with respect to the associated wavelength. The mechanical to electrical energy conversion has been performed in many different ways, such as linear generators and hydraulic mechanisms to provide a steady stream to a turbine (Pecher and Kofoed, 2017).

The efficiency maximization of PA-WECs has been vastly studied in recent years, as can be seen in Korde et al. (2016); Wang et al. (2018); Ringwood et al. (2020). Falnes (2002) establishes amplitude and phase conditions of the floater motion in order to satisfy this objective. Both conditions are derived from the maximum power transfer theorem (MPTT) for linear circuits (Desoer and Kuh, 1969). Two main optimal control approximations to fulfill these conditions are grouped by Ringwood et al. (2020): approximate complex conjugate control (ACC) and approximate velocity tracking (AVT). The former adjusts the mechanical impedance, and the latter aims to track the optimal trajectory for the floater motion.

This work compares three methods according to the ACC approach applied to a point absorber WEC based on the Archimedes wave swing (AWS) prototype experimentally tested as described in Prado et al. (2006). Since the structure of the WEC allows fulfilling the phase condition

---

<sup>\*</sup> This research is supported by the UNAM program for Master of Science and Doctorate studies in engineering, CEMIE-Océano, and CONACyT.

by tuning the natural frequency of oscillation of the floater dynamics, the discussed options seek to reach the amplitude condition by adjusting the mechanical damping through the force produced by the generator. The first method assumes a linear approximation of the nonlinear damping produced by the braking subsystems, the second imposes linear dynamics by compensating the nonlinear damping. Finally, the third is a proposal based on a variation for nonlinear resistive circuits of the MPPT, which has not been previously contemplated for the WEC under study. The three methods are implemented given the model of the floater motion and tested in MATLAB/Simulink under two scenarios: ideal monochromatic sea waves, and then irregular ones which emulate real conditions. In both scenarios a sensitivity analysis of the damping correction is also included. The results demonstrate that a better performance is obtained with the proposed third method followed by the first one in the presence of both regular and irregular sea waves.

## 2. WEC DESCRIPTION

In this work, the case study is a WEC based on the full-scale Archimedes wave swing prototype tested in Portugal in 2004 with experimental results reported by Prado et al. (2006). A picture of the system before its deployment on the sea bottom is shown in Fig. 1.



Fig. 1. The 2004 Archimedes wave swing prototype (Prado et al., 2006)

### 2.1 Operation Principle

This WEC is placed on the sea-bottom and is composed of an air-filled tank covered by a floating lid, which moves vertically inside a support structure (Beirao et al., 2007a; Prado et al., 2006; Prado, 2013). The motion of the floater is produced by the forces caused by the sea waves on the surface and the pressure of the enclosed air, as depicted in Fig. 2.

The structure of the WEC also includes two sets of water brakes for upward and downward motion. These subsystems provide appropriate damping in the presence

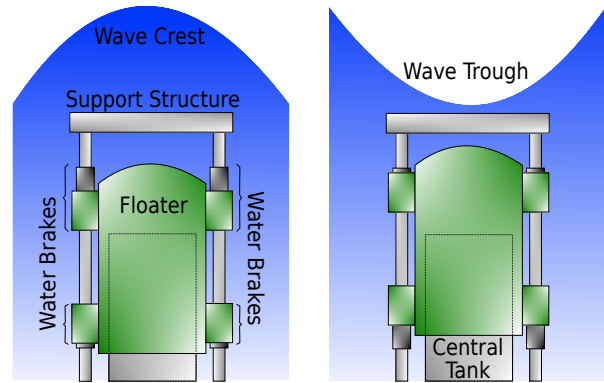


Fig. 2. Upward and downward motion of the floater produced by the sea waves and the enclosed air

of the extreme forces that act on the floater. On the other hand, the stiffness force is produced by the hydrostatic pressure on the top of the floater, the air enclosed inside the tank, an additional gas spring, and the weight of the floater. An important feature of this structure is the possibility of tuning the natural frequency of oscillation of the floater. This is performed by adjusting the average internal air pressure with a subsystem that regulates the water level inside the tank.

Furthermore, the electrical energy is obtained through a three-phase linear generator composed by a stator fixed inside the tank and a permanent magnet translator attached to the floater.

### 2.2 Floater Dynamics

From experimental results, the floater motion of an AWS prototype is modeled by Prado et al. (2006) as

$$\begin{aligned} \dot{x} &= v, \\ \dot{v} &= \frac{1}{m_t} \{ F_k(x) + F_b(v) + F_{gen} + F_w \}, \end{aligned} \quad (1)$$

where  $m_t$  is the total mass of the floater defined by its physical mass  $m_f$  and the effect of the radiation force  $m_{add}$ . Furthermore,  $x$  and  $v$  are the position and the velocity of the floater, respectively. In addition,

$$F_k(x) = -kx \quad (2)$$

is the stiffness force with a constant coefficient  $k$ ,

$$F_b(v) = -\beta v|v| \quad (3)$$

is the damping force with a constant coefficient  $\beta$ ,  $F_w$  is the excitation force produced by the sea wave, and  $F_{gen}$  is the force produced by the linear generator. Following Wu et al. (2008), the generator dynamics are neglected in this study as they are considerably faster than those of the floater.

### 2.3 Guidelines for Maximization of the Converted Energy

The energy converted by the WEC in a time interval  $[t_1, t_2]$  is given by

$$E = - \int_{t_1}^{t_2} F_{gen} v dt. \quad (4)$$

In order to shape  $F_{gen}$  for maximizing  $E$ , one assigns

$$F_{gen} = -k_g x + \varphi(v), \quad (5)$$

where the coefficient  $k_g \geq 0$  and the function  $\varphi(\cdot)$  are design parameters. With the purpose of adjusting both parameters, the phase and amplitude conditions established by Falnes (2002) are considered.

Firstly, the phase condition is described by

$$\frac{k_g + k}{m_t} = \omega_0^2, \quad (6)$$

where  $\omega_0$  is the angular frequency of the excitation force approximated as a regular (monochromatic) wave with amplitude  $F$ :

$$F_w = F \sin(\omega_0 t). \quad (7)$$

One can notice that the condition (6) implies synchronization of the phase of the floater velocity with the excitation force. Secondly, if (6) is satisfied in the presence of  $F_w$  given by (7) and by neglecting the harmonic distortion produced by the nonlinear term  $-\beta v|v|$  in (1) one can assume

$$\dot{v} + \frac{k + k_g}{m_t} x \approx 0. \quad (8)$$

Following Prado et al. (2006),  $k$  can be adjusted by varying the water level inside the central tank. Hence, for the sake of simplicity in this work it is considered  $k_g = 0$ . Then,  $F_{gen} = \varphi(v)$  represents the damping adjustment for the floater motion depicted in Fig. 3. In this diagram, the mechanical subsystem block represents the floater dynamics, and the electrical subsystem block represents the control system of the generator and its interaction to the power converter connected to the electric grid. Wu et al. (2008) describe a field-oriented control strategy in order to shape the generator force  $F_{gen}$  by tracking the reference  $F_{gen}^R$ .

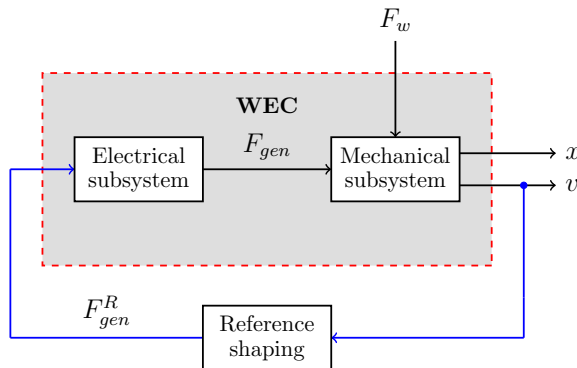


Fig. 3. Scheme for approximate complex conjugate control of the WEC

In this study, it is assumed that  $F_{gen} = F_{gen}^R$  as the generator dynamics are assumed to be considerably faster than those of the floater. Thus, the floater motion model can be reduced to the static relation

$$F_b(v) + F_{gen} = -F_w. \quad (9)$$

Thus, for the system (9) given the linear approximation of the damping force

$$F_b \approx -bv, \quad (10)$$

where  $b > 0$  is the approximate damping coefficient, the amplitude condition is given by

$$\varphi(v) = -bv. \quad (11)$$

Different approaches for computing  $b$  are presented in Beirao et al. (2007b); Gieske (2007); Wu et al. (2008).

The conditions (6) and (11) rely on the assumptions (7) and (10). Therefore, this work considers a relaxation of the latter in order to compare three different methods for designing  $F_{gen}$  as described in the following section.

### 3. METHODS FOR DAMPING ADJUSTMENT

This work compares three methods for adjusting the damping of the WEC to improve the energy conversion. The first considers a linear approximation of the damping produced by the brakes, the second imposes a linear dynamic, and the third is a proposal based on a variation of the MPTT for nonlinear circuits. These methods are described as follows.

#### 3.1 Linear Approximation (LA)

The simplest design of  $F_{gen}$  is obtained given the assumption (10). Under the conditions indicated above, one obtains

$$F_{gen} = -bv. \quad (12)$$

This result can be obtained from the maximum power transfer theorem (MPTT) for linear resistive circuits (Desoer and Kuh, 1969) applied to the system (9).

By relaxing the assumption (10), the total damping force in (1) is given by

$$F_b(v) + F_{gen} = -\beta v|v| - bv. \quad (13)$$

#### 3.2 Damping Linearization (DL)

Since the assumption (10) considers a linear damping of the floater motion, an alternative can be obtained by canceling the nonlinear damping through

$$F_{gen} = \beta v|v| - 2bv. \quad (14)$$

This method imposes linear dynamics for the floater motion, as the total damping force in (1) is given by

$$F_b(v) + F_{gen} = -2bv. \quad (15)$$

This is an intuitive choice since the harmonic distortion produced by the nonlinear damping term is canceled out.

#### 3.3 Nonlinear Damping Correction (NLD)

In this work a third option is formulated by taking into account the assumption (8) without avoiding the nonlinear damping. This proposal is derived from the variation of the MPTT for nonlinear resistive circuits presented in Wyatt and Chua (1983).

Given a monochromatic excitation force  $F_w = F \sin(\omega_0 t)$  from (4) and (5) with  $k_g + k = m_t \omega_0^2$  by neglecting the harmonic distortion produced by the nonlinear damping, the energy conversion maximization problem can be reduced to

$$v^* = \arg \min_v \int_{t_1}^{t_2} \varphi(v) v dt, \quad (16)$$

subject to (9) for  $t_2 \gg t_1$ . Following Wyatt and Chua (1983),  $v^*$  must satisfy

$$\varphi^*(v^*) = v \frac{\partial}{\partial v} F_b(v) \Big|_{v=v^*}. \quad (17)$$

Therefore, by considering (3) one can establish that the appropriate form of the generator force is given by

$$F_{gen} = -2\beta v|v| \quad (18)$$

and that the total damping force in (1) results

$$F_b(v) + F_{gen} = -3\beta v|v|. \quad (19)$$

#### 4. NUMERICAL SIMULATIONS

In order to compare the described methods for improving the converted energy, their performance was tested in Matlab/Simulink simulations with the values indicated in Table 1.

Table 1. WEC simulation parameters

Parameter	Value	Units
$m_t$	$0.6 \times 10^6$	kg
$k$	0.24	MN/m
$\beta$	1.42	MNs <sup>2</sup> /m <sup>2</sup>
$k_g$	0	N/m

Two scenarios were considered for the analysis. First, a regular wave with period  $2\pi/\omega_0 = 10$  s and  $F = 0.9$  MN is assigned for  $F_w$ . An irregular sea wave modeled according to the JONSWAP spectrum (Faltinsen, 1993) is then simulated. The approximate linear damping coefficient is computed as

$$b = \beta v_p, \quad (20)$$

where  $v_p$  is the steady-state amplitude of the floater velocity obtained from simulations with  $F_{gen} = 0$  and the monochromatic excitation force described above. The simulation of each method includes a sensitivity analysis by supposing uncertainty of the damping coefficient given by the parameter  $\alpha$  as follows:

- Linear approximation (LA)

$$F_{gen} = -(1 + \alpha)bv, \quad (21)$$

- Damping linearization (DL)

$$F_{gen} = \beta v|v| - 2(1 + \alpha)bv, \quad (22)$$

- Nonlinear damping (NLD)

$$F_{gen} = -2(1 + \alpha)\beta v|v|. \quad (23)$$

##### 4.1 Scenario A: Regular Sea Wave

The results in Fig. 4 show the converted energy in a 100 s time window with a regular sea wave obtained

from simulations by varying  $\alpha$  for each of the described methods. It can be seen that greater energy values are obtained with the NLD with small variations of  $\alpha$ . On the other hand, one can notice that the value of  $b$  computed from (20) provides a better performance with the LA compared with the DL.

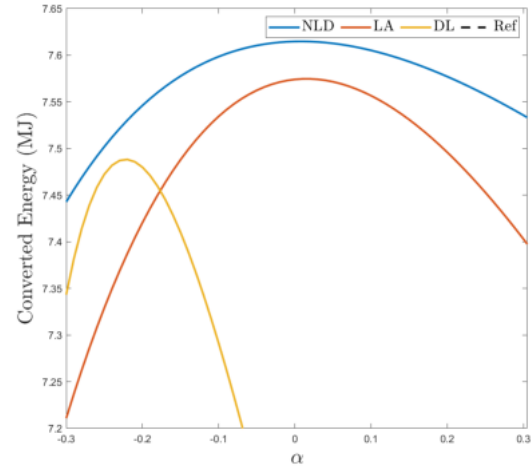


Fig. 4. Energy converted in a 100 s time window with different damping adjustments under a regular wave

The observations above can be complemented with the maximum values indicated in Table 2. The small variations of  $\alpha$  for NLD and LA can be related to the assumption given by (8), as the harmonic distortion caused by the nonlinear damping term is neglected. The results allow establishing that such an approximation provides an adequate performance for both NLD and LA. Moreover, the cancellation of the nonlinear term performed through the DL method has an important cost regarding the energy conversion and also requires further adjustment of  $b$ .

Table 2. Maximum converted energy value for each method with a regular sea wave

	LA	DL	NLD
$E_{max}$ (MJ)	7.58	7.49	7.62
$\alpha^*$	0.02	-0.22	0.01

In addition, the time evolution of the position and the velocity of the floater during a 20 s time window are shown in Fig. 5, with the values of  $\alpha$  that lead to greater energy conversion for each method. One can see in the plot of the floater velocity that the result with LA is closer to the one obtained with DL. As the latter cancels out the effect of the nonlinear term, one can establish that the harmonic distortion with LA is lower than that produced with NLD.

Furthermore, the time evolution of the generator force and the instantaneous converted power during the assigned 20 s time window is presented in Fig. 6. Since the action of the tested methods is restricted to the

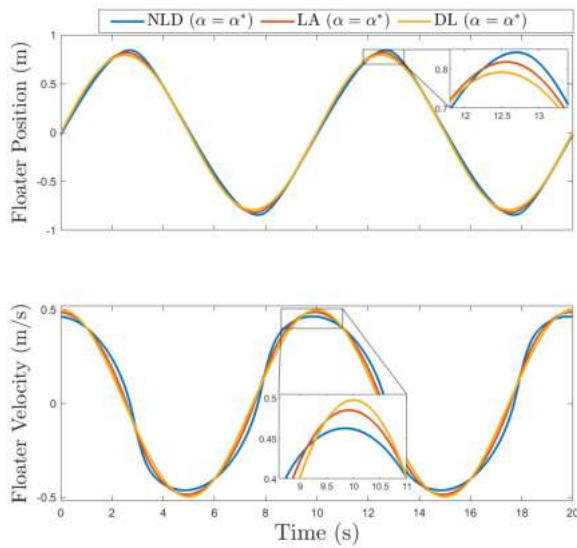


Fig. 5. Time evolution of the floater position and velocity under a regular wave

correction of the damping force through the generator, the instantaneous converted power remains positive along the operation of the converter. Despite the harmonic distortion with NLD that is noticeable in the time evolution of the position and velocity of the floater, one can also notice similar waveforms for the instantaneous converted power with the three methods. In spite of this result, one can foresee that for longer operation periods the differences regarding the converted energy become larger, which represents an important advantage for the NLD.

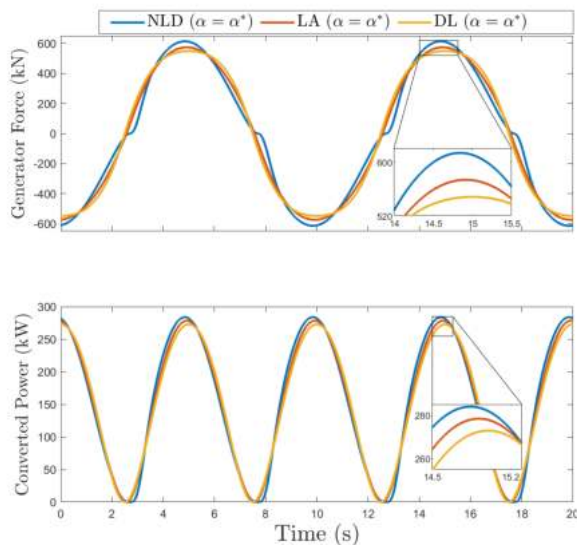


Fig. 6. Time evolution of the generator force and instantaneous converted power under a regular wave

#### 4.2 Scenario B: Irregular Sea Wave

Following (Faltinsen, 1993), the excitation force produced by an irregular sea wave is modeled as

$$F_w = \sum_{i=1}^N F_i \sin(\omega_i t + \phi_i), \quad (24)$$

where the values of the coefficients  $F_i$  are obtained from an approximation of the JONSWAP spectrum with a useful bandwidth around  $\omega_0 = 2\pi/10$  rad/s, random phase shifts  $\phi_i$ , and peak values around 0.9 MN.

The values of the converted energy obtained during a time window of 100 s with the three methods according to variations of  $\alpha$  are shown in Fig. 7. It can be seen that like the previous case the NLD provides greater energy conversion. It can also be seen, however, that the deviation represented by  $\alpha$  becomes larger in this scenario for all the three methods, as it is detailed in Table 3. Since more frequencies are present in the excitation force, the fulfillment of the assumption (8) becomes more complicated. Furthermore, additional harmonics are introduced by the nonlinear damping term that is compensated only by the DL.

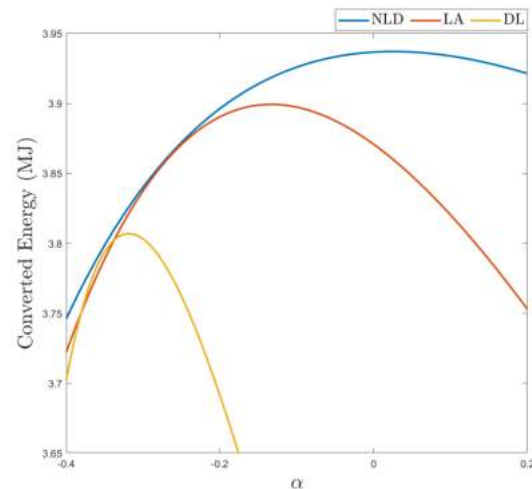


Fig. 7. Energy converted in a 100 s time window with different damping adjustments under an irregular wave

Table 3. Maximum converted energy value for each method with an irregular sea wave

	LA	DL	NLD
$E_{max}$ (MJ)	3.90	3.81	3.94
$\alpha^*$	-0.13	-0.32	0.02

The time evolution of the position and the velocity of the floater during a 20 s time window with the values of  $\alpha$  with greater efficiency for each method is shown in Fig. (8). Unlike the previous case, the harmonic distortion is not easily noticeable in the time domain. Nevertheless, it can be seen again that the LA gives results closer to

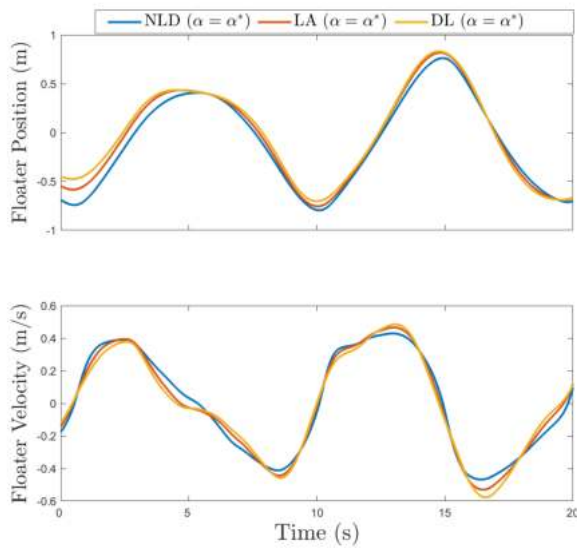


Fig. 8. Time evolution of the floater position and velocity under an irregular wave

those of DL, which imposes linear dynamics because of the nonlinear damping compensation.

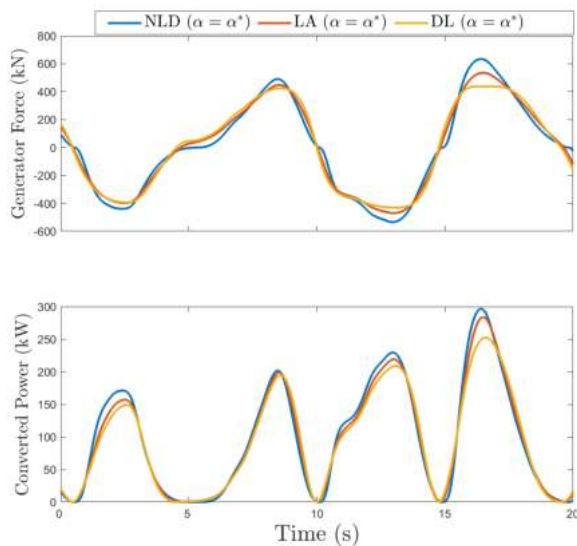


Fig. 9. Time evolution of the generator force and instantaneous converted power under an irregular wave

Finally, the time evolution of the generator force and the instantaneous converted power during the selected time window and  $\alpha$  values for each method is shown in Fig. 9. Again the instantaneous converted power remains positive since the generator force is shaped only for damping correction, and the waveforms of this feature obtained with all the three methods barely reflect the differences noticeable in the position and speed of the floater and the generator force. Even though the power produced with NLD shows instant values slightly greater

than those obtained with LA and DL, the difference becomes more significant for longer periods when the converted energy is compared.

## 5. CONCLUSIONS

Three damping adjustment methods for a WEC have been compared. The results show a better performance regarding energy conversion with the methods that preserve with the nonlinear behavior, with respect to the one that imposes linear dynamics over the floater motion. An approximate linear damping model has been shown to be useful for adjusting the total damping of the floater motion through the generator with the linear approximation method. The use of a more realistic nonlinear model, however, allowing the improvement the performance of the WEC, as noticed for longer operation periods.

Even though a degraded performance is obtained in the presence of irregular sea waves compared with regular ones, the required correction of the damping model is not a complicated task. Moreover, better linear approximations of the damping force can be obtained, allowing the reduction of further adjustments required by the linear approximation option. In addition, an optimal trajectory tracking strategy could improve the energy conversion as it may not rely on the natural frequency adjustment that depends on the proximity of the sea wave to a regular one.

The main difficulty for applying the discussed methods to a real WEC lies in the model of the damping force. In addition, the additional damping produced by the radiation force may have a more important effect on the floater dynamics for other WEC topologies.

Further research aims to maximize the energy converted by the WEC through robust control strategies such as model predictive and  $H_\infty$ , as well as by considering effects such as nonlinear stiffness and the harmonic distortion on the generator dynamics, which have been neglected in this study.

## REFERENCES

- Beirao, P., Mendes, M., Valério, D., and da Costa, J.S. (2007a). Control of the archimedes wave swing using neural networks. In *7th European Wave and Tidal Energy Conference*.
- Beirao, P., Valério, D., and da Costa, J.S. (2007b). Linear model identification of the archimedes wave swing. In *2007 International Conference on Power Engineering, Energy and Electrical Drives*, 660–665. IEEE.
- Desoer, C.A. and Kuh, E.S. (1969). *Basic circuit theory*. McGraw-Hill, Inc.
- Falnes, J. (2002). *Ocean Waves and Oscillating Systems: Linear Interaction including Wave-Energy Extraction*. Cambridge University Press, USA.
- Faltinsen, O. (1993). *Sea loads on ships and offshore structures*, volume 1. Cambridge university press.

- Gieske, P. (2007). *Model Predictive Control of a Wave Energy Converter: Archimedes Wave Swing*. Master's thesis, Delft University of Technology, Delft, Netherlands.
- Korde, U.A., Robinett, R.D., and Wilson, D.G. (2016). Wave-by-wave control in irregular waves for a wave energy converter with approximate parameters. *Journal of Ocean Engineering and Marine Energy*, 2(4), 501–519.
- Mork, G., Barstow, S., Kabuth, A., and Pontes, M. (2010). Assessing the global wave energy potential. In *ASME. International Conference on Offshore Mechanics and Arctic Engineering. 29th International Conference on Ocean, Offshore and Arctic Engineering*, volume 3, 447–454.
- Pecher, A. and Kofoed, J.P. (2017). *Handbook of Ocean Wave Energy*, volume 7. Springer International Publishing, Berlin, Germany.
- Prado, M. (2013). Case study of the Archimedes Wave Swing (AWS) direct drive wave energy pilot plant. In M. Mueller and H. Polinder (eds.), *Electrical Drives for Direct Drive Renewable Energy Systems*, volume 2, chapter 9, 195–218. Springer, Berlin/Heidelberg, Germany.
- Prado, M., Gardner, F., Damen, M., and Polinder, H. (2006). Modelling and test results of the Archimedes Wave Swing. *Proceedings of The Institution of Mechanical Engineers Part A-journal of Power and Energy - PROC INST MECH ENG A-J POWER*, 220, 855–868.
- Ringwood, J.V., Mérigaud, A., Faedo, N., and Fusco, F. (2020). An analytical and numerical sensitivity and robustness analysis of wave energy control systems. *IEEE Transactions on Control Systems Technology*, 28(4), 1337–1348.
- Wang, L., Isberg, J., and Tedeschi, E. (2018). Review of control strategies for wave energy conversion systems and their validation: the wave-to-wire approach. *Renewable and Sustainable Energy Reviews*, 81, 366 – 379. doi:<https://doi.org/10.1016/j.rser.2017.06.074>.
- Wu, F., Zhang, X., Ju, P., and Sterling, M.J.H. (2008). Modeling and control of aws-based wave energy conversion system integrated into power grid. *IEEE Transactions on Power Systems*, 23(3), 1196–1204.
- Wyatt, J. and Chua, L. (1983). Nonlinear resistive maximum power theorem, with solar cell application. *IEEE Transactions on Circuits and Systems*, 30(11), 824–828.